

# Near-Unity Coupling Efficiency of a Quantum Emitter to a Photonic Crystal Waveguide

M. Arcari,<sup>1</sup> I. Söllner,<sup>1,\*</sup> A. Javadi,<sup>1</sup> S. Lindskov Hansen,<sup>1</sup> S. Mahmoodian,<sup>1</sup> J. Liu,<sup>1</sup> H. Thyrrstrup,<sup>1</sup> E. H. Lee,<sup>2</sup>  
J. D. Song,<sup>2</sup> S. Stobbe,<sup>1</sup> and P. Lodahl<sup>1,†</sup>

<sup>1</sup>*Niels Bohr Institute, University of Copenhagen, Blegdamsvej 17, DK-2100 Copenhagen, Denmark*

<sup>2</sup>*Center for Opto-Electronic Convergence Systems, Korea Institute of Science and Technology, Seoul 136-791, Korea*

(Received 22 May 2014; published 29 August 2014)

A quantum emitter efficiently coupled to a nanophotonic waveguide constitutes a promising system for the realization of single-photon transistors, quantum-logic gates based on giant single-photon nonlinearities, and high bit-rate deterministic single-photon sources. The key figure of merit for such devices is the  $\beta$  factor, which is the probability for an emitted single photon to be channeled into a desired waveguide mode. We report on the experimental achievement of  $\beta = 98.43\% \pm 0.04\%$  for a quantum dot coupled to a photonic crystal waveguide, corresponding to a single-emitter cooperativity of  $\eta = 62.7 \pm 1.5$ . This constitutes a nearly ideal photon-matter interface where the quantum dot acts effectively as a 1D “artificial” atom, since it interacts almost exclusively with just a single propagating optical mode. The  $\beta$  factor is found to be remarkably robust to variations in position and emission wavelength of the quantum dots. Our work demonstrates the extraordinary potential of photonic crystal waveguides for highly efficient single-photon generation and on-chip photon-photon interaction.

DOI: 10.1103/PhysRevLett.113.093603

PACS numbers: 42.50.Ct, 42.50.Ex, 78.67.Hc, 81.05.Ea

The proposals of quantum communication [1] and linear-optics quantum computing [2] have been major driving forces for the development of efficient single-photon (SP) sources [3–5]. Furthermore, the access to photon nonlinearities that are sensitive at the SP level [6,7] would open for novel opportunities of constructing highly efficient deterministic quantum gates [7–13]. A single quantum emitter that is efficiently coupled to a photonic waveguide [14] would facilitate such a SP nonlinearity, enabling the realization of single-photon switches and diodes [7–9], as well as serve as a highly efficient single-photon source. Waveguide-based schemes offer highly efficient and broadband channeling of SPs into a directly usable propagating mode where even the photon detection can be integrated on chip [15]. The associated SP nonlinearity constitutes a very promising and robust alternative to the technologically demanding schemes based on the anharmonicity of the strongly coupled emitter-cavity system [16–19].

In the present work we consider a single quantum dot (QD) embedded in a photonic crystal waveguide (PCW). The important figure of merit is the  $\beta$  factor:

$$\beta = \frac{\Gamma_{wg}}{\Gamma_{wg} + \Gamma_{rad} + \Gamma_{nr}} = \frac{\Gamma_c - \Gamma_{uc}}{\Gamma_c}, \quad (1)$$

which gives the probability for a single exciton in the QD to recombine by emitting a single photon into the waveguide mode.  $\Gamma_{wg}$  and  $\Gamma_{rad}$  are the rate of decay of the QD into either the guided mode or nonguided radiation modes, whereas  $\Gamma_{nr}$  denotes the intrinsic nonradiative decay rate of the QD. The  $\beta$  factor is related to the single-emitter cooperativity  $\eta = \beta/(1 - \beta)$  [20]. Experimentally, the  $\beta$  factor can be obtained by recording the decay rate of a QD that is coupled to the waveguide  $\Gamma_c = \Gamma_{wg} + \Gamma_{rad} + \Gamma_{nr}$

and the rate of an uncoupled QD  $\Gamma_{uc} = \Gamma_{rad} + \Gamma_{nr}$  in the case where the difference between the total loss rates ( $\Gamma_{rad} + \Gamma_{nr}$ ) of the two QDs is negligible.

Recent proposals have indicated that the  $\beta$  factor in PCWs may approach unity [21,22]. However, measuring a near-unity  $\beta$  factor is experimentally challenging, because the reliable extraction of  $\Gamma_{uc}$  is not straightforward. A proper measurement of the  $\beta$  factor requires the precise determination of  $\Gamma_{uc}$  for a QD that is coupled to the waveguide. In previous work [23–27]  $\Gamma_{uc}$  was estimated either from QDs spectrally tuned to the band gap of the photonic crystal, or from QDs positioned outside the waveguide region (for a more detailed discussion of the previous experimental methods, see Ref. [28]). The drawback of both approaches is that the modifications in the coupling to the nonguided modes from the presence of the waveguide are not accounted for, which may lead to largely incorrect estimates of the  $\beta$  factor, as revealed by numerical simulations.

In the present work, the  $\beta$  factor is experimentally determined by comparing the decay rate of a QD coupled to the waveguide mode  $\Gamma_c$  to that of a very weakly coupled QD, which constitutes an upper bound of  $\Gamma_{uc}$ . One of the key differences to previous work is that both  $\Gamma_c$  and  $\Gamma_{uc}$  are obtained by directly detecting the propagating waveguide mode; hence, all measured QDs are spatially positioned in the waveguide. This guarantees that the spatial and spectral dependence of the coupling to radiation modes due to the presence of the PCW are correctly taken into account, which is essential for the analysis. The validity of our experimental method is confirmed by numerical simulations of the position and frequency dependence of  $\Gamma_{rad}$  in the PCW structure. We experimentally demonstrate a SP channelling

efficiency of  $\beta = 98.43\% \pm 0.04\%$  for a QD in a PCW, which significantly surpasses previously reported results exploiting atoms [20,38], nitrogen vacancy centers [39], single molecules [3], or quantum dots [4,23,40] as the photon sources in photonic-waveguide structures. This corresponds to a single-emitter cooperativity  $\eta = 62.7 \pm 1.5$ , which surpasses by almost 1 order of magnitude previously reported values both with QDs [23] and atoms [20]. Such a high coupling efficiency matches the level achievable with superconducting microwave circuits, widely considered one of the most mature platforms for scalable quantum-information processing available today, and will lead to novel opportunities for photonic quantum-information processing [41].

A near-unity  $\beta$  factor PCW SP source is illustrated in Fig. 1(a): a deterministic train of SPs in the waveguide can be obtained since the excited QD will emit a photon into the waveguide with probability  $\beta$ , while out-of-plane photon loss is strongly suppressed. High  $\beta$  factors are achievable due to the combination of two effects: a broadband Purcell enhancement of the rate  $\Gamma_{wg}$  of coupling into the waveguide and the strong suppression of the loss rate  $\Gamma_{rad}$  due to the photonic crystal membrane structure. Different physical systems have been proposed for obtaining a large  $\beta$  factor: plasmonic nanowires rely on the Purcell enhancement thereby increasing  $\Gamma_{wg}$  [40], while dielectric nanowires [4,39] mainly suppress the coupling to radiation modes, i.e., decrease  $\Gamma_{rad}$ . In PCWs the beneficial combination of the Purcell enhancement of the PCW mode and the pronounced reduction of radiation modes enables a near-unity  $\beta$  factor.

In PCWs the Purcell enhancement is proportional to the group index or slow-down factor  $n_g = c/v_g$ , where  $c$  is the speed of light in vacuum. The group velocity of light,  $v_g$ , is the slope of the waveguide band, see Fig. 1(b), which decreases at the waveguide band edge. We have measured  $n_g > 50$  close to the band edge, leading to expected Purcell factors close to 10 [21]. For the method used to extract the  $n_g$ , see Ref. [28]. Furthermore, the photonic crystal band gap strongly inhibits the in-plane radiative loss rate of the dipole emitter, while total internal reflection limits the decay by out-of-plane radiation.

The calculated position dependent  $\beta$  factor for a dipole emitter in proximity of the band edge ( $n_g = 58$ ) and close to the light line ( $n_g = 5$ ) is shown in Fig. 1(e). The fraction of the emission coupled to the waveguide and to the radiation modes can be determined numerically, and  $\Gamma_{wg}$  and  $\Gamma_{rad}$  are obtained by multiplying by the measured average radiative decay rate of QDs in a homogeneous medium  $\Gamma_{hom} = 0.91 \pm 0.08 \text{ ns}^{-1}$ . The measured average nonradiative decay rate is  $\Gamma_{nr} = 0.030 \pm 0.018 \text{ ns}^{-1}$ . In the slow-light regime ( $n_g = 58$ ),  $\beta$  factors exceeding 95% are predicted for dipole positions close to the field maxima of the waveguide mode [Fig. 1(d)]. In agreement with previous results [21,22], even outside the slow-light regime ( $n_g = 5$ ),  $\beta$  factors exceeding 90% are predicted for many positions in the waveguide, illustrating the very broadband coupling. The position dependence of the  $\beta$  factor, that is displayed in

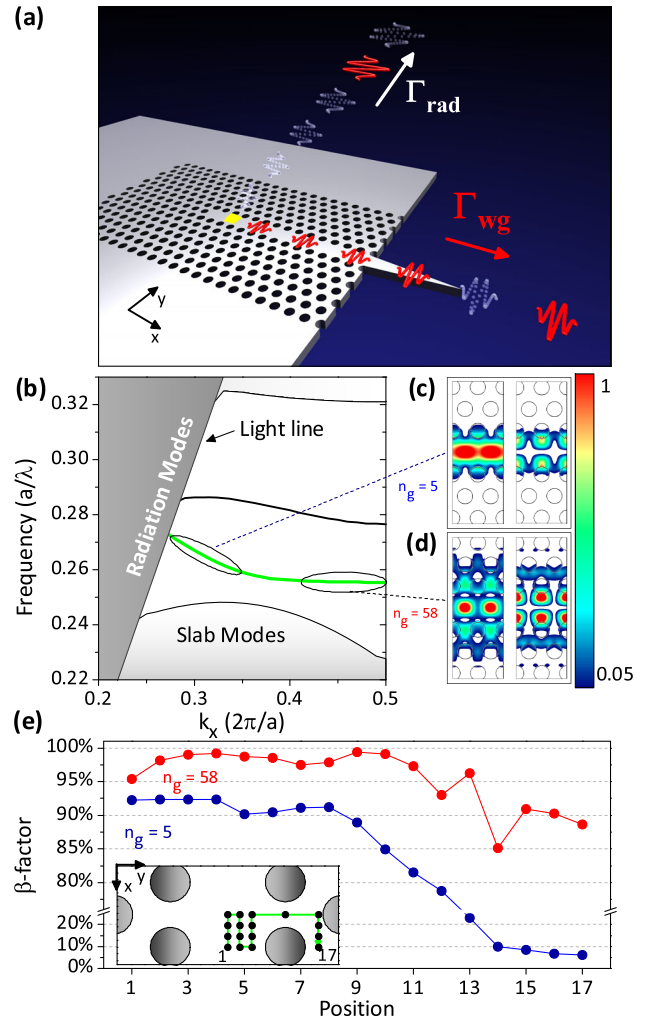


FIG. 1 (color online). (a) Illustration of the device. A train of single-photon pulses (red pulses) are emitted from a triggered QD (yellow trapezoid). The photons are channeled with near-unity probability into the waveguide mode with a rate  $\Gamma_{wg}$  while the weak rate  $\Gamma_{rad}$  of coupling to radiation modes implies that only very few photons are lost. The guided photons can be efficiently extracted from the waveguide through a tapered mode adapter. (b) Projected TE band structure of the PCW studied in the experiments displaying even (green) and odd (black) waveguide modes in the band gap. In the experiment only the even mode is studied. The shaded area of the dispersion diagram corresponds to the continuum of radiation modes. (c),(d) Electric field intensity spatial profiles  $|E_x|^2$  (right) and  $|E_y|^2$  (left) for two different spectral regions of the waveguide mode corresponding to two different group indices  $n_g$ . (e) Maximum  $\beta$  factor of the two orthogonal dipoles at  $n_g = 58$  (red) and  $n_g = 5$  (blue) calculated at the positions indicated in the inset. The maximum  $\beta$  factor is the quantity measured in decay-dynamics experiments.

Fig. 1(e), is determined by the spatial mode profiles of the guided modes shown in Figs. 1(c)–1(d).

We investigate light emission from a single layer of self-assembled InAs QDs embedded in a GaAs PCW (see Ref. [28] for sample description). In order to efficiently collect the photons from the propagating waveguide mode,

either second-order Bragg gratings [42] or inverse tapered mode adapters [43] are used. A numerical study of the coupling efficiency of the two outcoupling methods is presented in Ref. [28]. Scanning-electron microscope images of typical devices are shown in Figs. 2(a)–2(c). Since the mode adapters are designed to work in the regime

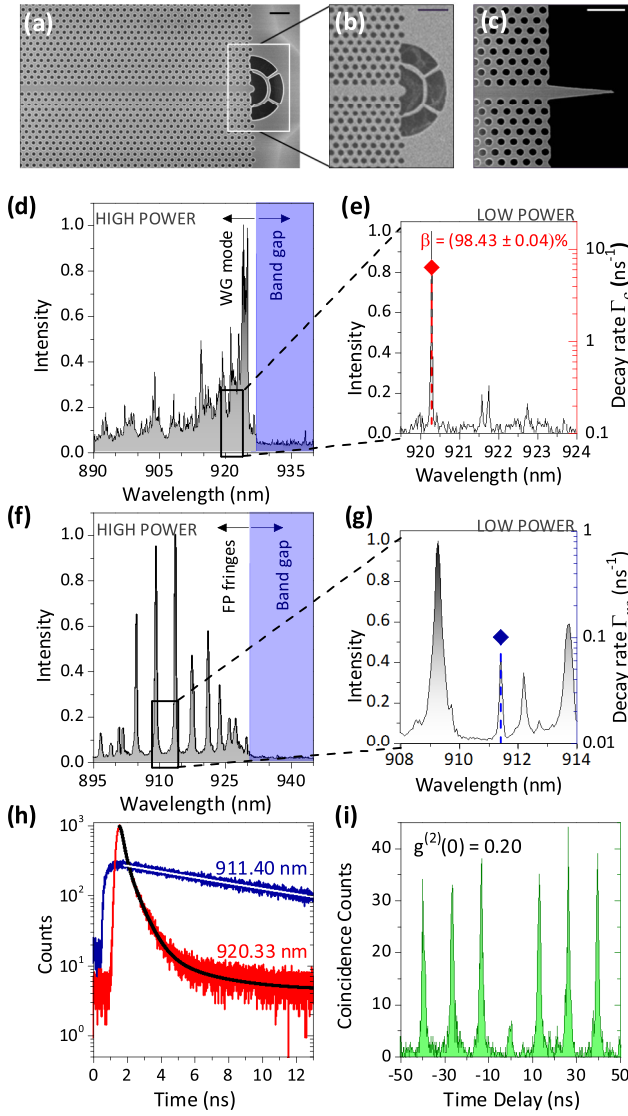


FIG. 2 (color online). (a) Scanning-electron microscope image of a typical device. QDs are excited in an area centered on the PCW, and the resulting emission is collected either from (b) the grating or (c) the tapered mode adapter. The scale bars correspond to 1  $\mu\text{m}$ . (d) High-power emission spectrum displaying the mode of the high- $n_g$  waveguide section for a grating structure with weakly reflecting ends. (e) Low-power spectrum with the corresponding decay rate  $\Gamma_c$  and  $\beta$  factor for a QD that is efficiently coupled to the waveguide. (f) High-power emission spectrum for a low- $n_g$  waveguide section with a highly reflective grating mode adapter. (g) Low power spectrum and decay rate  $\Gamma_{uc}$  of a QD spectrally in between two FP resonances. (h) Decay curves of QD lines shown in (e) (red curve) and in (g) (blue curve). (i) Measured autocorrelation function of the QD in (e).

of low  $n_g$ , a transition region is introduced in the photonic crystal in order to couple from the high- $n_g$  waveguide mode into the low- $n_g$  mode [44]. The length of the high- $n_g$  region varies between 5.1 and 8.3  $\mu\text{m}$  for different samples; a short sample length is chosen to eliminate the formation of Anderson-localized modes [45], which are detrimental for obtaining a high waveguide transmission. The averaged extinction length for light propagation in similar waveguides was measured to be  $l \approx 30 \mu\text{m}$  [46].

Figure 2(d) shows a high-power photoluminescence spectrum of the waveguide mode collected from the grating under nonresonant excitation, which is used to characterize the waveguide samples. The applied power is approximately 2 orders of magnitude higher than the saturation power of single excitons; i.e., single QD lines cannot be distinguished in this case. The spectrum displays a cutoff at 925 nm due to the waveguide band edge and a transmission bandwidth of 35 nm. Similar spectra were obtained when collecting the emission from the inverse tapers. We also investigated waveguide structures where a change in parameters of the gratings led to high reflectivity and the formation of sharp Fabry-Pérot (FP) resonances within the waveguide bandwidth, as shown in Fig. 2(f). In these structures the coupling to the waveguide mode for QDs spectrally positioned in between two resonances is expected to be very weak due to the inhibition of the local density of optical states, implying that the measured  $\Gamma_{uc}$  is close to the lower limit of  $\Gamma_{rad} + \Gamma_{nr}$ . This is confirmed by the experiment, as discussed below.

Time-resolved photoluminescence spectroscopy is employed to characterize the dynamics of QDs in a 20 nm range, blue-detuned from the band edge cutoff. For each QD line, decay curves are measured at an excitation power level well below saturation, see Fig. 2(h). For details on how the decay curves are modeled, see Ref. [28].

We extract Purcell-enhanced decay rates of up to  $\Gamma_c = 6.28 \pm 0.15 \text{ ns}^{-1}$  in the high- $n_g$  waveguide sections [Fig. 2(e)] and inhibited decay rates down to  $\Gamma_{uc} = 0.098 \pm 0.001 \text{ ns}^{-1}$  between two FP resonances in the low- $n_g$  waveguide section [Fig. 2(g)]. This corresponds to  $\beta = 98.43\% \pm 0.04\%$ . The uncertainty of this value has been extracted from the error of the fit. We have measured the  $\beta$  factor for a total of 71 different QDs within a 20 nm range in both the samples with grating and taper mode adapters, and the results are shown in Fig. 3. In both samples, the  $\beta$  factors are above 90% for most of the QDs in a 5 nm range close to the edge of the band-gap region, and we measure  $\beta$  factors above 90% for QDs up to 20 nm spectrally detuned from the band edge, thus highlighting the robustness of these devices. These results agree very well with the theoretical predictions of Fig. 1(e), which shows that QDs with a  $\beta$  factor above 90% can be expected even at  $n_g = 5$  for specific positions in the waveguide. In the following we will focus on the highest  $\beta$  factors found for QDs in the proximity of the band edge. The SP nature of the emission lines is confirmed by recording the normally ordered second order intensity correlation function  $g^{(2)}(\tau) = \langle : \hat{I}(t) \hat{I}(t + \tau) : \rangle / \langle \hat{I}(t) \rangle^2$

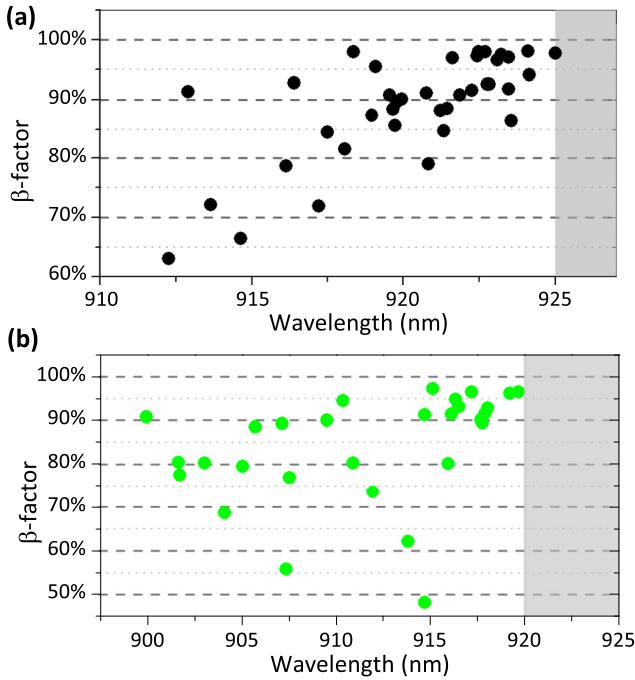


FIG. 3 (color online). (a)  $\beta$  factors measured on the grating samples and (b) on the samples with tapered waveguides. In both figures, the band gap region above the waveguide cutoff is indicated in grey.

under pulsed excitation. An example of a measurement for the highest  $\beta$  factor QD of Fig. 2(e) is shown in Fig. 2(i), where  $g^{(2)}(0) = 0.20$  is found at 0.63 of saturation power. Since the criterion for single-photon emission is  $g^{(2)}(0) < 0.5$ , our result clearly demonstrates single-photon emission from the QD. For further details about the analysis of  $g^{(2)}(\tau)$ , see Ref. [28]. Even stronger antibunching has been observed for QDs in spectrally very clean regions of the waveguide mode reaching  $g^{(2)}(0) < 0.05$  at excitation powers below the saturation level.

The applied method for extracting the  $\beta$  factor by comparing  $\Gamma_c$  and  $\Gamma_{uc}$  of two different QDs is valid since the variation of the total loss rate  $\Gamma_{rad} + \Gamma_{nr}$  between different QDs is small. Indeed, the variations in  $\Gamma_{nr}$  over the wavelength range of relevance can be neglected [47] while the spatial variation of  $\Gamma_{rad}$  has been calculated as shown in Fig. 4(b) for an efficiently ( $n_g = 58$ ) and weakly coupled ( $n_g = 7$ ) QD. The chosen values of  $n_g$  correspond to the cases of the QDs shown in Figs. 2(e) and 2(g). For most positions,  $\Gamma_{rad}$  is found to be lower than the experimental estimate based on  $\Gamma_{rad} = \Gamma_{uc} - \Gamma_{nr}$  [indicated by the dashed line in Fig. 4(a)], which is expected since residual coupling to the waveguide will increase the rate. At a few spatial positions in Fig. 4(a), the predicted  $\Gamma_{rad}$  is found to be higher than the experimental rate. However, as displayed in Fig. 4(b) these are not the positions where the large Purcell-enhanced decay rates observed in the experiment appear [experimental values indicated by the dashed line in Fig. 4(b)], and we can thus exclude that the QDs with the

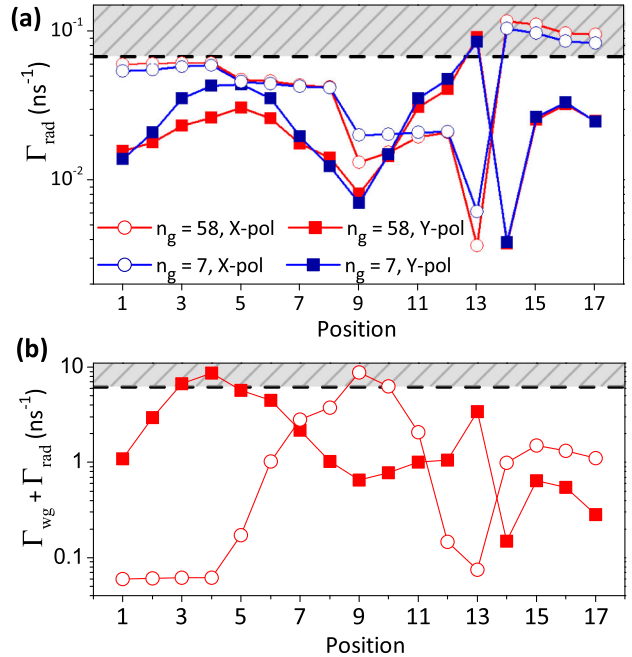


FIG. 4 (color online). (a) Position-dependent radiative loss rate for a y-polarized (squares) or x-polarized (circles) dipole emitting at either  $n_g = 58$  in the high- $n_g$  waveguide section (red data) or  $n_g = 7$  in the low- $n_g$  waveguide section (blue data). The shaded region indicates where the predicted  $\Gamma_{rad}$  is above the experimentally extracted value of  $0.068 \pm 0.008 \text{ ns}^{-1}$ . (b) Calculated radiative rate as a function of position for a dipole aligned along the y direction (squares) or the x direction (circles) and emitting at  $n_g = 58$ . The corresponding emitter positions are indicated in the inset of Fig. 1(e). The shaded region indicates where the predicted decay rate is above the experimentally extracted value of  $6.28 \pm 0.15 \text{ ns}^{-1}$  for the high- $\beta$ -factor QD.

highest  $\beta$  factor are positioned here, implying that the record-high  $\beta$  factors constitute conservative estimates.

In conclusion, we have for the first time unambiguously measured a near-unity  $\beta$  factor in a PCW, and have shown the robustness of  $\beta$  with respect to the wavelength and the spatial position of the emitter in the PCW. This result proves the high potential of PCWs to achieve strong on-chip light-matter coupling between a QD and a propagating mode, which opens the way for the realization of transistors and gates for deterministic quantum information processing. To this end highly coherent photon emission is required, and decoherence processes have been found to be slow for quasiresonant excitation of QDs in photonic crystals [48,49] and could be further extended by applying true resonant excitation [50–52]. Furthermore, a highly efficient SP source can be built by optimizing the outcoupling mode adapters of our structures, making the source immediately applicable for linear-optics quantum-computing experiments.

We acknowledge fruitful discussion with Anders S. Sørensen. We thank Sara Ek for her input into the design of the tapered structures. We gratefully acknowledge financial support from the Danish Council for Independent

Research (Natural Sciences and Technology and Production Sciences) and the European Research Council (ERC consolidator grant ALLQUANTUM). I. S. and M. A. contributed equally to this work.

\*sollner@nbi.ku.dk

†lodahl@nbi.ku.dk; <http://quantum-photonics.nbi.ku.dk>

- [1] C. H. Bennett and G. Brassard, in *Proceedings of the IEEE International Conference on Computers, Systems and Signal Processing, Bangalore, India* (IEEE, New York, 1984), pp. 175.
- [2] E. Knill, R. Laflamme, and G. J. Milburn, *Nature (London)* **409**, 46 (2001).
- [3] K. G. Lee, X. W. Chen, H. Eghlidi, P. Kukura, R. Lettow, A. Renn, V. Sandoghdar, and S. Götzinger, *Nat. Photonics* **5**, 166 (2011).
- [4] J. Claudon, J. Bleuse, N. S. Malik, M. Bazin, P. Jaffrennou, N. Gregersen, C. Sauvan, P. Lalanne, and J.-M. Gérard, *Nat. Photonics* **4**, 174 (2010).
- [5] O. Gazzano, M. P. Almeida, A. K. Nowak, S. L. Portalupi, A. Lemaître, I. Sagnes, A. G. White, and P. Senellart, *Phys. Rev. Lett.* **110**, 250501 (2013).
- [6] P. R. Rice and H. J. Carmichael, *IEEE J. Quantum Electron.* **24**, 1351 (1988).
- [7] D. E. Chang, A. S. Sørensen, E. A. Demler, and M. D. Lukin, *Nat. Phys.* **3**, 807 (2007).
- [8] J. Gao, F. W. Sun, and C. W. Wong, *Appl. Phys. Lett.* **93**, 151108 (2008).
- [9] Y. Shen, M. Bradford, and J. T. Shen, *Phys. Rev. Lett.* **107**, 173902 (2011).
- [10] W. Chen, K. M. Beck, R. Bucker, M. Gullans, M. D. Lukin, H. Tanji-Suzuki, and V. Vuletic, *Science* **341**, 768 (2013).
- [11] J. Hwang, M. Pototschnig, R. Lettow, G. Zumofen, A. Renn, S. Götzinger, and V. Sandoghdar, *Nature (London)* **460**, 76 (2009).
- [12] Q. A. Turchette, C. J. Hood, W. Lange, H. Mabuchi, and H. J. Kimble, *Phys. Rev. Lett.* **75**, 4710 (1995).
- [13] T. Peyronel, O. Firstenberg, Q.-Y. Liang, S. Hofferberth, A. V. Gorshkov, T. Pohl, M. D. Lukin, and V. Vuletić, *Nature (London)* **488**, 57 (2012).
- [14] J. T. Shen and S. Fan, *Opt. Lett.* **30**, 2001 (2005).
- [15] G. Reithmaier, S. Lichtmannecker, T. Reichert, P. Hasch, K. Müller, M. Bichler, R. Gross, and J. J. Finley, *Sci. Rep.* **3**, 1901 (2013).
- [16] D. Englund, A. Majumdar, M. Bajcsy, A. Faraon, P. Petroff, and J. Vučković, *Phys. Rev. Lett.* **108**, 093604 (2012).
- [17] T. Volz, A. Reinhard, M. Winger, A. Badolato, K. J. Hennessy, E. L. Hu, and A. Imamoğlu, *Nat. Photonics* **6**, 605 (2012).
- [18] H. Kim, R. Bose, T. C. Shen, G. S. Solomon, and E. Waks, *Nat. Photonics* **7**, 373 (2013).
- [19] K. M. Birnbaum, A. Boca, R. Miller, A. D. Boozer, T. E. Northup, and H. J. Kimble, *Nature (London)* **436**, 87 (2005).
- [20] T. G. Tiecke, J. D. Thompson, N. P. de Leon, L. R. Liu, V. Vuletić, and M. D. Lukin, *Nature (London)* **508**, 241 (2014).
- [21] V. S. C. Manga Rao and S. Hughes, *Phys. Rev. B* **75**, 205437 (2007).
- [22] G. Lecamp, P. Lalanne, and J. P. Hugonin, *Phys. Rev. Lett.* **99**, 023902 (2007).
- [23] T. Lund-Hansen, S. Stobbe, B. Julsgaard, H. Thyrrstrup, T. Sünder, M. Kamp, A. Forchel, and P. Lodahl, *Phys. Rev. Lett.* **101**, 113903 (2008).
- [24] S. J. Dewhurst, D. Granados, D. J. P. Ellis, A. J. Bennett, R. B. Patel, I. Farrer, D. Anderson, G. A. C. Jones, D. A. Ritchie, and A. J. Shields, *Appl. Phys. Lett.* **96**, 031109 (2010).
- [25] H. Thyrrstrup, L. Sapienza, and P. Lodahl, *Appl. Phys. Lett.* **96**, 231106 (2010).
- [26] T. Ba Hoang, J. Beetz, L. Midolo, M. Skacel, M. Lermer, M. Kamp, S. Höfling, L. Balet, N. Chauvin, and A. Fiore, *Appl. Phys. Lett.* **100**, 061122 (2012).
- [27] A. Laucht *et al.*, *Phys. Rev. X* **2**, 011014 (2012).
- [28] See Supplemental Material at <http://link.aps.org/supplemental/10.1103/PhysRevLett.113.093603> for additional data, description, and analysis of results in this Letter, which contains Refs. [29–37].
- [29] N. A. Wasley, I. J. Luxmoore, R. J. Coles, E. Clarke, A. M. Fox, and M. S. Skolnick, *Appl. Phys. Lett.* **101**, 051116 (2012).
- [30] Y. Chen, T. R. Nielsen, N. Gregersen, P. Lodahl, and J. Mork, *Phys. Rev. B* **81**, 125431 (2010).
- [31] K. H. Madsen, P. Kaer, A. Kreiner-Møller, S. Stobbe, A. Nysteen, J. Mørk, and P. Lodahl, *Phys. Rev. B* **88**, 045316 (2013).
- [32] C. Santori, D. Fattal, J. Vučković, G. S. Solomon, E. Waks, and Y. Yamamoto, *Phys. Rev. B* **69**, 205324 (2004).
- [33] J. Vučković, D. Fattal, C. Santori, G. S. Solomon, and Y. Yamamoto, *Appl. Phys. Lett.* **82**, 3596 (2003).
- [34] M. Bayer *et al.*, *Phys. Rev. B* **65**, 195315 (2002).
- [35] A. J. Bennett *et al.*, *Nat. Phys.* **6**, 947 (2010).
- [36] Q. Wang, S. Stobbe, and P. Lodahl, *Phys. Rev. Lett.* **107**, 167404 (2011).
- [37] C.-M. Simon *et al.*, *Phys. Rev. Lett.* **106**, 166801 (2011).
- [38] E. Vetsch, D. Reitz, G. Sagué, R. Schmidt, S. T. Dawkins, and A. Rauschenbeutel, *Phys. Rev. Lett.* **104**, 203603 (2010).
- [39] T. M. Babinec, B. J. M. Hausmann, M. Khan, Y. Zhang, J. R. Maze, P. R. Hemmer, and M. Lončar, *Nat. Nanotechnol.* **5**, 195 (2010).
- [40] A. V. Akimov, A. Mukherjee, C. L. Yu, D. E. Chang, A. S. Zibrov, P. R. Hemmer, H. Park, and M. D. Lukin, *Nature (London)* **450**, 402 (2007).
- [41] P. Lodahl, S. Mahmoodian, and S. Stobbe, [arXiv:1312.1079](https://arxiv.org/abs/1312.1079).
- [42] A. Faraon, I. Fishman, D. Englund, N. Stoltz, P. Petroff, and J. Vuckovic, *Opt. Express* **16**, 12 154 (2008).
- [43] Q. V. Tran, S. Combrié, P. Colman, and A. De Rossi, *Appl. Phys. Lett.* **95**, 061105 (2009).
- [44] J. P. Hugonin, P. Lalanne, T. P. White, and T. F. Krauss, *Opt. Lett.* **32**, 2638 (2007).
- [45] L. Sapienza, H. Thyrrstrup, S. Stobbe, P. D. Garcia, S. Smolka, and P. Lodahl, *Science* **327**, 1352 (2010).
- [46] P. D. García, S. Smolka, S. Stobbe, and P. Lodahl, *Phys. Rev. B* **82**, 165103 (2010).
- [47] J. Johansen, B. Julsgaard, S. Stobbe, J. M. Hvam, and P. Lodahl, *Phys. Rev. B* **81**, 081304 (2010).
- [48] S. Laurent *et al.*, *Appl. Phys. Lett.* **87**, 163107 (2005).
- [49] K. H. Madsen, S. Ates, J. Liu, A. Javadi, S. M. Albrecht, I. Yeo, S. Stobbe, and P. Lodahl, [arXiv:1402.6967](https://arxiv.org/abs/1402.6967).
- [50] Y.-M. He, Y. He, Y.-J. Wei, D. Wu, M. Atatüre, C. Schneider, S. Höfling, M. Kamp, C.-Y. Lu, and J.-W. Pan, *Nat. Nanotechnol.* **8**, 213 (2013).
- [51] C. Matthiesen, A. N. Vamivakas, and M. Atatüre, *Phys. Rev. Lett.* **108**, 093602 (2012).
- [52] H. S. Nguyen, G. Sallen, C. Voisin, Ph. Roussignol, C. Diederichs, and G. Cassabois, *Appl. Phys. Lett.* **99**, 261904 (2011).